David A. Dowe
Massimo Fioranelli
Paolo Pavone *Editors*

Imaging Coronary Arteries

Second edition

In collaboration with
Roberto Leo

With a collection
of clinical cases

Springer

Imaging Coronary Arteries

David A. Dowe
Massimo Fioranelli
Paolo Pavone

Editors

Imaging Coronary Arteries

Second edition

In collaboration with
Roberto Leo

With a collection
of clinical cases

Springer

Editors
David A. Dowe
Coronary CTA Program Director
Atlantic Medical Imaging
Galloway, NJ, USA

Massimo Fioranelli
Head of Heart Center
Casa di Cura Mater Dei
Rome, Italy
Scientific Director of the
Centro Studi in Scienze della Vita
"Guglielmo Marconi" University
Rome, Italy

Paolo Pavone
Radiology Department
Casa di Cura Mater Dei
Rome, Italy

ISBN 978-88-470-2681-0 ISBN 978-88-470-2682-7 (eBook)
DOI 10.1007/978-88-470-2682-7
Springer Milan Heidelberg New York Dordrecht London

Library of Congress Control Number: 2012951304

Cover design: Ikona S.r.l., Milan, Italy
Typesetting: C & G di Cerri e Galassi, Cremona, Italy
Printing and binding: Grafiche Porpora, Segrate (MI), Italy

Springer-Verlag Italia S.r.l., Via Decembrio 28, 20137 Milan

Springer is a part of Springer Science+Business Media (www.springer.com)

Preface to the Second Edition

Coronary artery disease (CAD) is one of the leading causes of death in developed countries, yet for many years the prediction of clinical events has been reliant upon methods with substantial drawbacks. Non-invasive, indirect examinations such as Framingham risk factors, thorough clinical examination, EKG and the treadmill test yield valid information but certainly do not provide a safe and complete assessment of the presence of CAD. Even nuclear medicine techniques provide only indirect information on the presence of disease and are not always specific. On the other hand, direct imaging of the coronary arteries using selective coronary angiography, possible since the 1960s, is an invasive procedure that is not well tolerated by patients; this remains true despite progress in catheter and guidewire design and the development of stenting procedures that allow diagnosis and therapy within the same clinical setting.

Coronary CT angiography has been proposed relatively recently as an alternative to selective coronary angiography. Progress in equipment design has transformed what was originally a research tool into a reliable, clinically accepted procedure that is easy to perform. The widely debated issue of X-ray dose has now been partially solved as we have moved from an absolutely unacceptable dose of 25-30 mSv to a routine dose of 3-5 mSv or even 1 mSv. Furthermore, a reduction in the acquisition time has permitted the contrast medium dose to be consistently lowered from 120-150 ml to 40-50 ml. Acceptance of coronary CT angiography continues to grow, although there is still no consensus on its role as a non-invasive diagnostic test in intermediate risk patients.

Looking beyond coronary CT angiography, magnetic resonance angiography (MRA) of the coronary arteries has been the subject of considerable clinical research but has not yet entered general clinical practice despite advances on various fronts. A further significant advance is the use of techniques that allow imaging of the coronary arterial walls during selective coronary angiography (intravascular ultrasound, IVUS, and optical coherence tomography, OCT); this approach is improving our understanding of CAD and providing better evidence of the type of vascular wall involvement.

This new edition of Imaging Coronary Arteries fully reflects the latest advances in coronary CT angiography and includes extensively revised or entirely new chapters on IVUS, catheter angiography and OCT as well as discussion of the role of nuclear imaging and MRA. A further very significant

new feature is the inclusion of 74 clinical cases that will serve to illustrate the wide range of clinical cases encountered in daily practice and to demonstrate the utmost importance of correlation of clinical and imaging findings.

The editors would like to express their gratitude to all who have been involved in the preparation of this edition, which will without doubt be of great interest to radiologists, cardiologists, CT technologists and others. Special thanks are due to Dr. Marco Rengo, Dr. Carlo Nicola De Cecco, Dr. Davide Bellini, Dr. Damiano Caruso and Dr. Marco Maria Maceroni for their support in the preparation of the updated chapters 2, 3, 4, 8 and 9.

November 2012

David A. Dowe
Massimo Fioranelli
Paolo Pavone

Preface to the First Edition

Coronary CT angiography (CTA) is rapidly changing the patient-care algorithms used to detect coronary artery disease, as well as the approach we take in risk-factor assessment and in the triage of patients. The rapid adoption of coronary CTA into clinical practice has been fueled by significant yearly advances in CT technology, which have improved the spatial and temporal resolution of this technique while simultaneously decreasing radiation exposure.

The growing utilization of coronary CTA has created a need for comprehensive didactic texts that explain the numerous applications of this new technology with respect to the pathophysiology of coronary artery disease, while also providing information on the approach to patients who have undergone previous bypass surgery or percutaneous coronary intervention. I believe this book accomplishes both of these goals, and does so in a reader-friendly format. The image quality of the many figures that accompany each chapter is excellent and reflects the use of state of the art technology. The techniques described for plaque detection and characterization represent the current thinking pervasive in the coronary CTA community. The comprehensive reference list at the end of the book offers the reader a wealth of resources for further study.

There is no doubt that this book will be popular with radiologists, cardiologists, CT technologists and anyone else seeking to acquire a comprehensive understanding of coronary artery disease and its depiction using coronary CTA.

Galloway, October 2008 David A. Dowe, MD

Contents

1 **Clinical Anatomy of the Coronary Circulation** 1
Massimo Fioranelli, Carlo Gonnella, Stefano Tonioni, Fabrizio D'Errico and Mariantonietta Carbone

2 **Basic Techniques in the Acquisition of Cardiac Images with CT** 13
Paolo Pavone

3 **CT Examination of the Coronary Arteries** 21
Paolo Pavone

4 **Image Reconstruction** 29
Paolo Pavone

5 **Coronary Pathophysiology** 41
Mara Piccoli, Serafino Orazi, Giovanna Giubilato and Massimo Fioranelli

6 **Clinical Classification of Coronary Artery Disease: Who Should Be Treated?** 47
Damien Casagrande, Jean-Jacques Goy, Mario Togni, Jean Christophe Stauffer and Stéphane Cook

7 **Intravascular Ultrasound: From Gray-Scale to Virtual Histology** 53
Giuseppe M. Sangiorgi, Luigi Politi, Chiara Leuzzi, Luigi Mattioli, Fabiana Rollini and Massimo Fioranelli

8 **Identification and Characterization of the Atherosclerotic Plaque Using Coronary CT Angiography** 63
Paolo Pavone, David A. Dowe and Roberto Leo

9 **Coronary CT Angiography: Evaluation of Stenosis and Occlusion** 71
Paolo Pavone and Roberto Leo

10 Current Strategies in Cardiac Surgery 85
Andrea Montalto and Francesco Musumeci

11 Coronary CT Angiography: Evaluation of Coronary Artery Bypass Grafts 91
Carlo Nicola De Cecco, Gorka Bastarrika and Marco Rengo

12 Coronary Stents 101
Enrica Mariano, Giuseppe M. Sangiorgi and Massimo Fioranelli

13 CT Angiography of Coronary Stents 115
Gorka Bastarrika, Carlo Nicola De Cecco and U. Joseph Schoepf

14 X-Ray Exposure in Coronary CT Angiography 131
Paolo Pavone and Roberto Leo

15 Optical Coherence Tomography in the Cathlab 137
Francesco Prati and Luca Di Vito

16 Triple Rule Out: the Use of Cardiac CT in the Emergency Room 147
Giulio Speciale and Vincenzo Pasceri

17 Contraindications to Coronary CT Angiography 153
David A. Dowe

18 Prognostic Value of Coronary CT 157
Bruno Pironi, Antonio Lucifero and Massimo Fioranelli

19 Clinical Cases 165
David A. Dowe, Paolo Pavone and Massimo Fioranelli

Index 259

Contributors

Gorka Bastarrika Cardiothoracic Imaging Division, Department of Medical Imaging, Sunnybrook Health Sciences Centre, Toronto, Canada

Mariantonietta Carbone Interventional Cardiovascular Unit, San Carlo Hospital, Rome, Italy

Damien Casagrande Cardiology Service, Hôpital Cantonal, Fribourg, Switzerland

Stéphane Cook Cardiology Service, Hôpital Cantonal, Fribourg, Switzerland

Carlo Nicola De Cecco Department of Radiological Sciences, Oncology and Pathology, University of Rome "La Sapienza" Polo Pontino, Latina, Italy

Fabrizio D'Errico Interventional Cardiovascular Unit, San Carlo Hospital, Rome, Italy

Luca Di Vito CLI Foundation, Centro per la Lotta contro l'Infarto, Rome, Italy

David A. Dowe Coronary CTA Program Director, Atlantic Medical Imaging, Galloway, NJ, USA

Massimo Fioranelli Head of Heart Center, Casa di Cura Mater Dei, Rome, Italy. Scientific Director of the Centro Studi in Scienze della Vita, "Guglielmo Marconi" University, Rome, Italy

Giovanna Giubilato Heart Center, Casa di Cura Mater Dei, Rome, Italy

Carlo Gonnella Cardiology Department, "San Carlo di Nancy" Hospital, Rome, Italy

Jean-Jacques Goy Cardiology Service, Hôpital Cantonal, Fribourg, Switzerland

Roberto Leo Internal Medicine, University of Rome Tor Vergata, Rome, Italy

Chiara Leuzzi Interventional Cardiology, Policlinico Universitario, Modena, Italy

Antonio Lucifero Heart Center, Casa di Cura Mater Dei, Rome, Italy

Enrica Mariano Interventional Cardiology Unit, "Tor Vergata" University, Rome, Italy

Luigi Mattioli Department of Cardiology, Cardiac Cath Lab, "Tor Vergata" University, Rome, Italy

Andrea Montalto Department of Cardiac Surgery and Transplantation, San Camillo Hospital, Rome, Italy

Francesco Musumeci Department of Cardiac Surgery and Transplantation, San Camillo Hospital, Rome, Italy

Serafino Orazi Head of Cardiology Department, Ospedale Civile di Rieti, Rieti, Italy

Vincenzo Pasceri Interventional Cardiology, San Filippo Neri Hospital, Rome, Italy

Paolo Pavone Radiology Department, Casa di Cura Mater Dei, Rome, Italy

Mara Piccoli Cardiology Unit, Policlinico "Luigi di Liegro", Rome, Italy

Bruno Pironi Interventional Cardiology, "M.G. Vannini" Hospital, Rome, Italy

Luigi Politi Interventional Cardiology, Policlinico Universitario, Modena, Italy

Francesco Prati Interventional Cardiology, San Giovanni Hospital, Rome, Italy

Marco Rengo Department of Radiological Sciences, Oncology and Pathology, University of Rome "La Sapienza" Polo Pontino, Latina, Italy

Fabiana Rollini Interventional Cardiology, Policlinico Universitario, Modena, Italy

Giuseppe M. Sangiorgi Interventional Cardiology, University of Roma Tor Vergata, Policlinico Casilino, Rome, Italy

U. Joseph Schoepf Department of Radiology and Radiological Science, Division of Cardiology, Department of Medicine, Medical University of South Carolina, Charleston, South Carolina, USA

Giulio Speciale Chief Interventional Cardiology, San Filippo Neri Hospital, Rome, Italy

Jean Christophe Stauffer Cardiology Service, Hôpital Cantonal, Fribourg, Switzerland

Mario Togni Cardiology Service, Hôpital Cantonal, Fribourg, Switzerland

Stefano Tonioni Cardiology Department, "San Carlo di Nancy" Hospital, Rome, Italy

Clinical Anatomy of the Coronary Circulation

1

Massimo Fioranelli, Carlo Gonnella, Stefano Tonioni, Fabrizio D'Errico and Mariantonietta Carbone

1.1 Introduction

The classification of the American Heart Association, which divides the coronary arteries into 15–16 segments, is often used in the evaluation of the coronary anatomy with multi-slice computed tomography (Fig. 1.1) [1-5]. In this chapter, a more complex classification is used, as it provides a more detailed anatomic picture. We begin with a brief review of the coronary anatomy.

The right coronary artery (RCA) takes origin from the right aortic sinus of Valsalva and then divides to form two terminal branches, the posterior descending artery (PDA) and the posterolateral (PLV) branches. Along its course, the RCA gives off several branches: the sinus node artery, right ventricular (RV) branches, acute marginal (AM) branch, and the atrioventricular node artery.

The left coronary artery (LCA) arises from the left aortic sinus of Valsalva; the left main (LM) branch of the LCA ends in a bifurcation, giving rise to the left anterior descending artery (LAD) and the left circumflex artery (LCx). Sometimes a third ramus intermedius is present between these two branches.

The LAD gives off septal (SP) and diagonal (DIAG) branches and ends at the apex of the heart, sometimes reaching the posterior interventricular groove. The LCx has two or three obtuse marginal branches (OM), before either terminating or, in the case of left-dominant or balanced circulation, giving off a posterolateral branch or ending in the posterior atrioventricular groove.

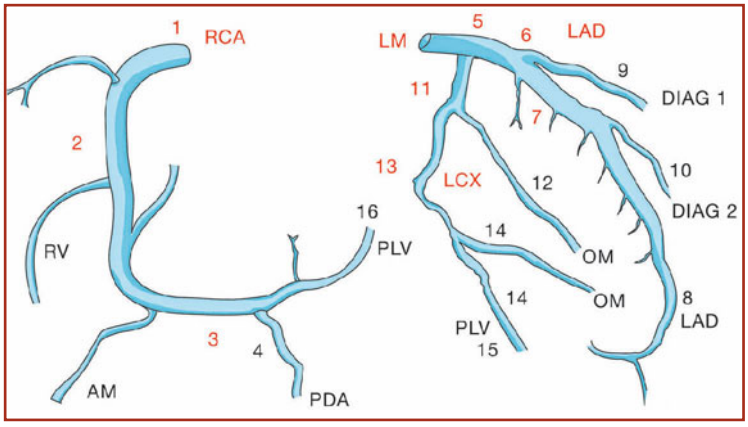

Fig. 1.1 Classification of the American Heart Association. *RC* right coronary artery, *RV* right ventricular branch, *AM* acute marginal branch, *PLV* posterolateral ventricular branch, *PDA* posterior descending artery, *LCA* left coronary artery, *LM* left main artery, *LAD* left anterior descending artery, *DIAG 1* first diagonal branch, *DIAG 2* second diagonal branch, *LCx* left circumflex artery, *OM* obtuse marginal branches

C. Gonnella (✉)
Cardiology Department
"San Carlo di Nancy" Hospital, Rome, Italy
e-mail: carlo.gonnella@tiscali.it

D.A. Dowe, M. Fioranelli and P. Pavone (eds.), *Imaging Coronary Arteries*,
DOI: 10.1007/978-88-470-2682-7_1, © Springer-Verlag Italia 2013

1.2 Angiographic Anatomy of the Coronary Circulation

The classification proposed in the Bypass Angioplasty Revascularization Investigation (BARI) trial reported by Alderman and Stadius (1992) divides the coronary arteries into 29 segments (Fig. 1.2).

The coronary trees have two principal components: the *subepicardial system* consists of the arteries and veins that course and ramify on the surface of the heart; the *intramyocardial system* comprises their perforating branches.

The subepicardial system is formed by the right and left coronary arteries, arising from the right and left aortic sinus of Valsalva, respectively. The RCA is divided into three segments. The first segment (BARI 1) extends from the coronary ostium to the first RV branch; if the latter is not present, the segment is usually identified between the ostium and the acute margin of the heart. The second segment (BARI 2) extends from the first RV branch to the acute margin of the heart, which usually coincides with the origin of the AM branch (BARI 10). This vessel is the most constant branch of the RCA and it runs on the surface of the free wall of the right ventricle in the direction of the apex, at an angle proportional to the proximity of its origin. The third segment (BARI 3) begins at the acute margin of the heart and courses to the origin of the PDA (BARI 4), at the level of the crux cordis. At this level, in right-dominant circulation (85% of cases), the RCA divides into two terminal branches, the PDA and PLV branches (BARI 5),

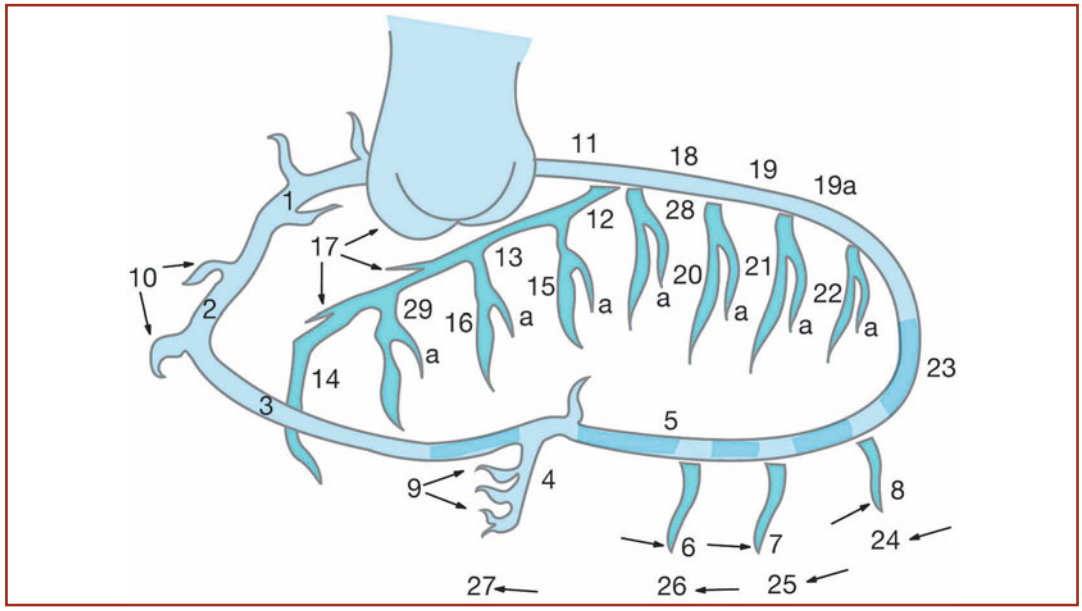

Fig. 1.2 Classification of the BARI Study Group: The coronary arteries are divided into 29 segments: *1* Proximal segment of the right coronary artery (RCA), *2* middle segment of the RCA, *3* distal segment of the RCA, *4* posterior descending artery (PDA), *5* posterolateral branch of the RCA (PLV), *6* first posterolateral branch of the RCA, *7* second posterolateral branch of the RCA, *8* third posterolateral branch of the RCA, *9* inferior septal branches, *10* acute marginal branches of the RCA, *11* left main of the left coronary artery (LM), *12* proximal segment of the left anterior descending artery (LAD), *13* middle segment of the LAD, *14* distal segment of the LAD, *15* first diagonal branch (DIAG), *15a* lateral first diagonal branch, *16* second diagonal branch, *16a* lateral second diagonal branch, *17* septal branches of the LAD (SP), *18* proximal segment of the left circumflex artery (LCx), *19* middle segment of the LCx, *19a* distal segment of the LCx, *20* first obtuse marginal branch (OM), *20a* lateral first obtuse marginal branch, *21* second obtuse marginal branch, *21a* lateral second obtuse marginal branch, *22* third obtuse marginal branch, *22a* lateral third obtuse marginal branch, *23* LCx continuing as the left atrioventricular branch, *24* first left posterolateral branch, *25* second left posterolateral branch, *26* third left posterolateral branch, *27* left posterior descending artery (PD) (in left-dominant circulation), *28* ramus intermedius, *28a* lateral ramus intermedius, *29* third diagonal branch, *29a* lateral third diagonal branch

perfusing the diaphragmatic wall of the left ventricle. In the remaining 15% of cases, the circulation may be left-dominant or balanced: in left-dominant circulation, the PLV and PDA originate from the LCx; in balanced circulation, the PDA originates from the RCA, and the PLV from the LCx.

The concept of dominance is defined by the relationship between the RCA and LCx, according to the origin of the PDA and in relation to the arterial supply of the inferior wall of the left ventricle, but independent of the extent of the circulatory system.

The PDA, also called the posterior interventricular branch, with its septal branches (BARI 9), is the most important branch of the RCA; it courses in the homonymous groove without reaching the apex of the heart, which is usually supplied by the recurrent branch of the LAD. The PLV immediately originates after the PDA, at the level of the crux cordis. It courses along the posterior atrioventricular sulcus, branching with its collateral vessels (BARI 6–8) at the diaphragmatic and inferioposterior walls of the left ventricle.

The RCA furnishes smaller branches such as the conus artery, sinus node artery, RV branches, and atrioventricular node artery (Fig. 1.3). The conus artery is the first vessel originating from the RCA. In 40% of the cases it directly originates from the right aortic sinus or from the aorta. The sinus node artery arises from the RCA (two-thirds of the cases); in 25% of cases, it may originate from the LCx, while in 10% the two vessels arise from both coronary arteries. The RV branches originate in the second segment of the RCA and run along the surface of the RV, anterior to the interventricular groove. The number of these branches varies greatly and is inversely proportional to the diameter of such vessels. In nearly all of the cases of right-dominant circulation and in 75% of the cases of balanced circulation, the atrioventricular node artery arises at the end of the third segment of the RCA. Its location is important in the angiographic identification of the crux cordis. In individuals with left-dominant circulation, it originates from the distal segment of the LCx. At the level of Koch's triangle is the subendocardial artery, situated between the septal cuspid of the tricuspid valve and the coronary sinus; it furnishes branches to the posterior interventricular septum and the atrioventricular node.

The LCA arises from the left aortic sinus, at a higher level than the RCA, and is divided into

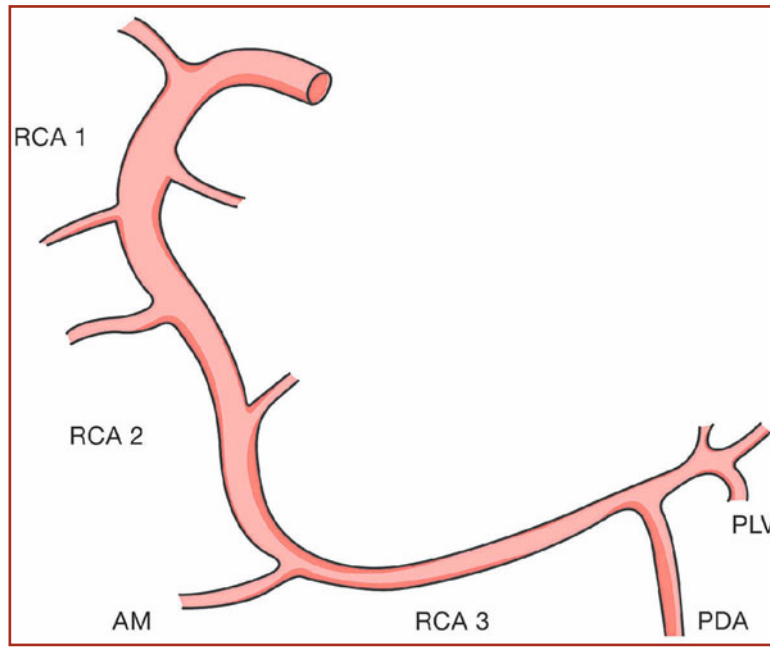

Fig. 1.3 Right coronary artery in left anterior oblique (LAO) view. *RCA* Right coronary artery (segments 1–3), *AM* acute marginal branch, *PLV* posterolateral branch, *PDA* posterior descending artery

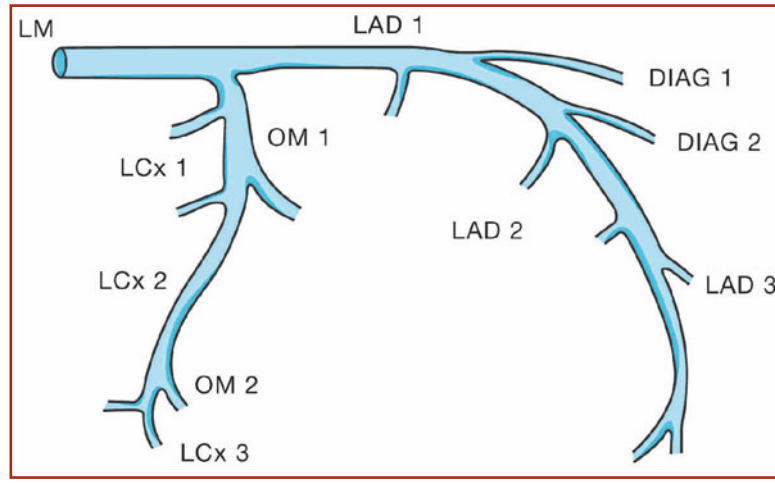

Fig. 1.4 Left coronary artery in caudal right anterior oblique (RAO) view. *LM* Left main artery, *LAD* left anterior descending artery (segments 1–3), *DIAG 1* first diagonal branch, *DIAG 2* second diagonal branch, *LCx* left circumflex artery (segments 1–3), *OM 1* first obtuse marginal branch, *OM 2* second obtuse marginal branch

three segments (Fig. 1.4). The LM branch of the LCA (BARI 11), also called the left main coronary artery (LMCA), extends for a varying length (generally 2 cm, diameter 3–6 mm) from the ostium to the bifurcation of the LAD and LCx. In 30–37% of the cases, the LM artery gives off three branches, one of which, the ramus intermedius (BARI 28), runs toward the apex and supplies the anterolateral wall of the left ventricle.

The LAD is the most constant, in origin and distribution, among all the coronary vessels. It originates from the LM artery and runs in the anterior interventricular groove to the apex of the heart. In 70% of the cases, the LAD extends up to the posterior interventricular groove such that it furnishes branches for perfusion of the inferior interventricular septum and the apex; otherwise, these arise along the length of the PDA. The first segment of the LAD (BARI 12) runs from the bifurcation of the LM artery to the origin of the first septal branch (SP, BARI 17). The second segment (BARI 13) extends from the origin of the first SP to the origin of the third septal or second DIAG branch. The third segment (BARI 14) ends at the apex, surrounding and sometimes traveling up to the posterior wall. When the third SP or second DIAG branch is not identified, the end of the second segment of the LAD is conventionally defined as the half-length between the first SP and the apex. The LAD furnishes branches for the anterior interventricular septum and the anterolateral wall of the left ventricle. There are generally three SP branches and they originate at right angles from the LAD.

The first SP branch is constant in its origin and course; thus, it is important to identify its passage between the proximal and middle segments of the LAD. Some segments may run intramyocardially but generally they develop caudally, along the interventricular septum, and supply the proximal two-thirds of the anterior septum. The second and third SP branches are more variable, with narrow diameters; they supply the distal third of the anterior septum. There are usually three DIAG branches (BARI 15, 16–29), each of which originates at an acute angle from the LAD; their pathway is to the anterolateral wall of the left ventricle. The diameter of these vessels is inversely proportional to the number of branches.

The LCx develops from the LM artery and runs in the posterior atrioventricular groove; after a short tract under the left atrium, it continues in the left posterior atrioventricular groove and contacts the mitral annulus. The LCx splits into three segments. The first (BARI 18) extends from the origin to the first marginal branch (OM, BARI 20). If the first OM is absent or not clearly identifiable, the zone of transition among the first and second segments is conventionally identified by a point corresponding to the half-length between the origin of the LCx and the origin of the second OM (BARI 21). The second segment (BARI 19) runs from the origin of the first OM to

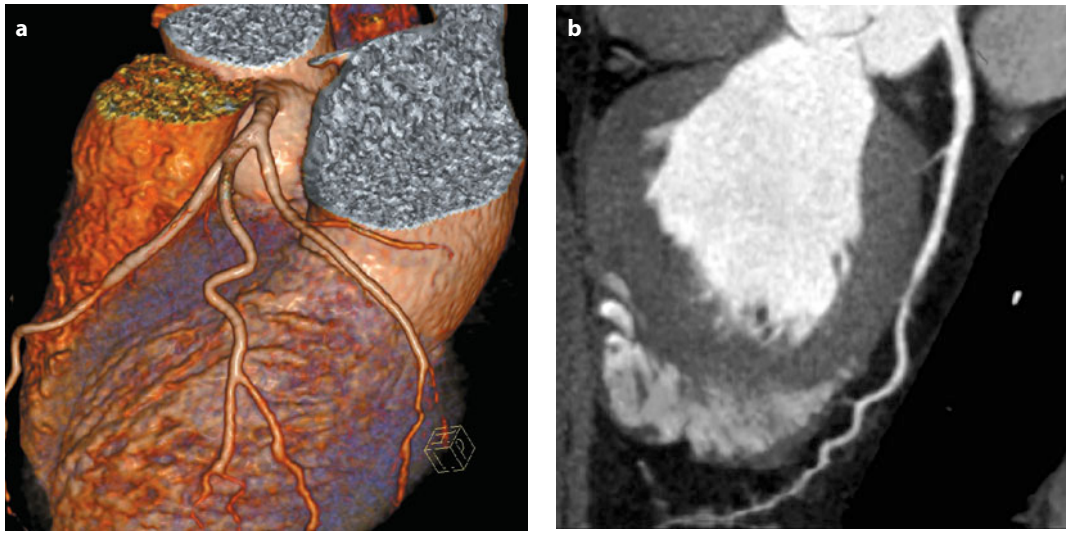

Fig. 1.5a, b Myocardial bridging of the left anterior descending artery reduces the arterial diameter

the origin of the second OM. If the second marginal branch is absent, the zone of transition is defined by the half-length between the origin of the first OM and the point where the circumflex artery terminates. The third segment (BARI 19a), in right-dominant circulation, extends from the origin of the second OM to the termination point of the vessel; in left-dominant or balanced circulation, to the point of origin of the left ventricular branch or the posterolateral branch in the posterior atrioventricular groove (BARI 23). In left-dominant circulation, the LCx gives rise to the left ventricular branch or PLV, with its side branches (BARI 24–26) and to the PDA (BARI 27), with its septal branches (BARI 9).

The LCx gives rise to the sinus node artery, left atrial branch, and marginal branches. In 25% of the cases, the sinus node artery arises from the proximal segment of the LCx, near the ostium. The atrial branch originates at the end of the proximal segment and runs to the inferoposterior wall of the left atrium. Of the three OM branches, the first one is usually larger and constant; it terminates on the posterolateral wall of the left ventricle toward the apex. Its development is inversely proportional both to the extent of the RCA on the posterolateral surface of the left ventricle and to the number and development of the diagonal branches of the LAD.

1.3 Intramyocardial Vascularization and the Venous Circulation

After oxygen and nutritional substrates have been extracted by the myocardium, a portion of the desaturated blood is transported directly into the ventricles through the Thebesian veins. Nevertheless, most of the blood, through the venules and myocardial veins, goes to the epicardial veins, which drain in the coronary sinus, located in the inferoposterior region of the right atrium.

The epicardial arteries are muscular vessels with a wall thickness of about 100 μm; they are made up of three overlapping layers: intima, media, and adventitia. These arteries, which transport oxygenated blood to the arteries, arterioles, and capillaries, traverse the surface of the heart covered by epicardium or sometimes by subepicardial adipose tissue. Muscular bridges of variable length, in which the epicardial vessels become intramyocardial, are present in 5–22% of the cases at the anterior LAD and in 86% in the other coronary arteries (Fig. 1.5).

Normal embryological development of the coronary circulation involves the formation of collateral vessels that link the different sections of the arterial circulation. The collateral circulation consists of four types of vessels: intramyocardial vessels originating from the same vessel (intracoronary

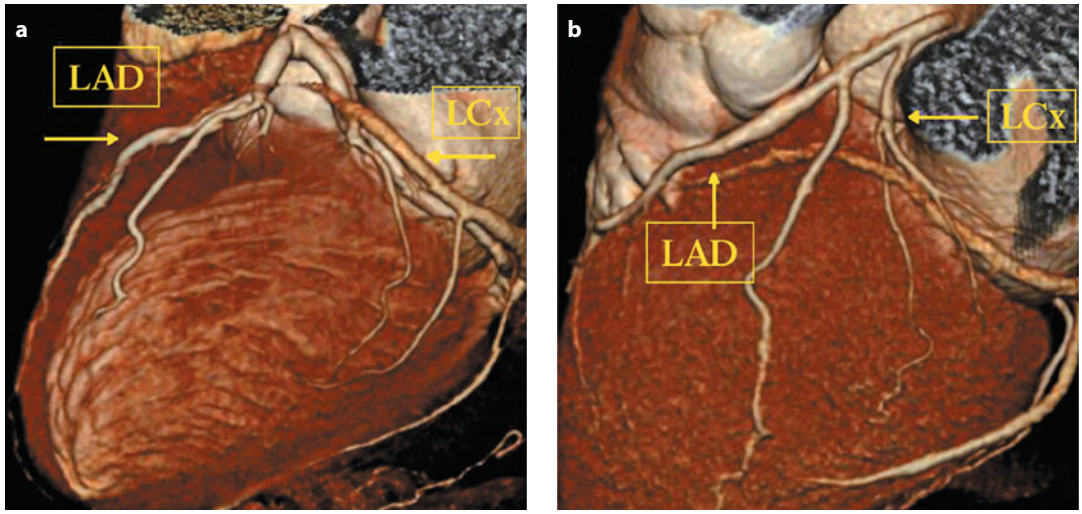

Fig. 1.6 a Hypertrophic left circumflex artery (*LCx*). **b** Hypoplastic LCx. *LAD* Left anterior descending artery

circulation), intramyocardial vessels originating from two or more coronary arteries (intercoronary circulation), atrial vessels connecting with the vasa vasorum of the aorta or other arteries (extracardiac circulation), and intramyocardial vessels that directly communicate with the ventricles (arteriolar luminal circulation). In the normal adult myocardium, the collateral circulation consists of small-caliber vessels (< 50 m in diameter) that contribute only marginally to coronary flow. In the presence of obstruction or myocardial ischemia, the diameter of the collateral vessels expands to 200–600 μm; the growth of a medial layer allows a significant quantity of blood flow. The development of collaterals results in the formation of connections among proximal and distal segments of a vessel crossing a stenosis.

1.4 Variability of the Coronary Artery Circulation

The native coronary artery circulation is highly variable. This is in contrast to other arterial vascular districts, which have a constant, readily identifiable anatomy, such as the carotid or iliac-femoral arteries, where, except for differences of caliber, the morphology, origin, and anatomic course are the same between individuals. Variations in the coronary arteries include the type of dominance, differences in caliber, and alternative branch morphologies. This aspect of the coronary circulation must be kept in mind during diagnostic evaluation of the arteries, to avoid considering an artery that is small and poorly developed as a stenosis.

The variability of the coronary circulation is such that two patients rarely have the same coronary vascular anatomy. In this context, the use of terminology such as "strongly developed branch" or "hypoplastic vessel" identifies the development of the vessel but does not denote the presence or absence of atherosclerotic lesions. For example, in some patients, the course and caliber of the LCx are highly developed, while in others the artery may be small and perfuses only a small portion of the myocardium. These differences are compensated for by the development of other vessels, which balance the perfusion of a myocardial region by a hypoplastic artery perfusion. The morphology of an artery and the extent of the territory it perfuses are very important considerations in therapeutic planning. The larger the myocardial region perfused by an artery, the greater the justification for a myocardial revascularization procedure in the presence of a critical stenosis.

As shown in Figure 1.6, there are some cases in which the LAD is more developed than the LCx, but in other situations the LCx is more developed and perfuses the largest part of the left ventricle. The caliber of the branches originating from these

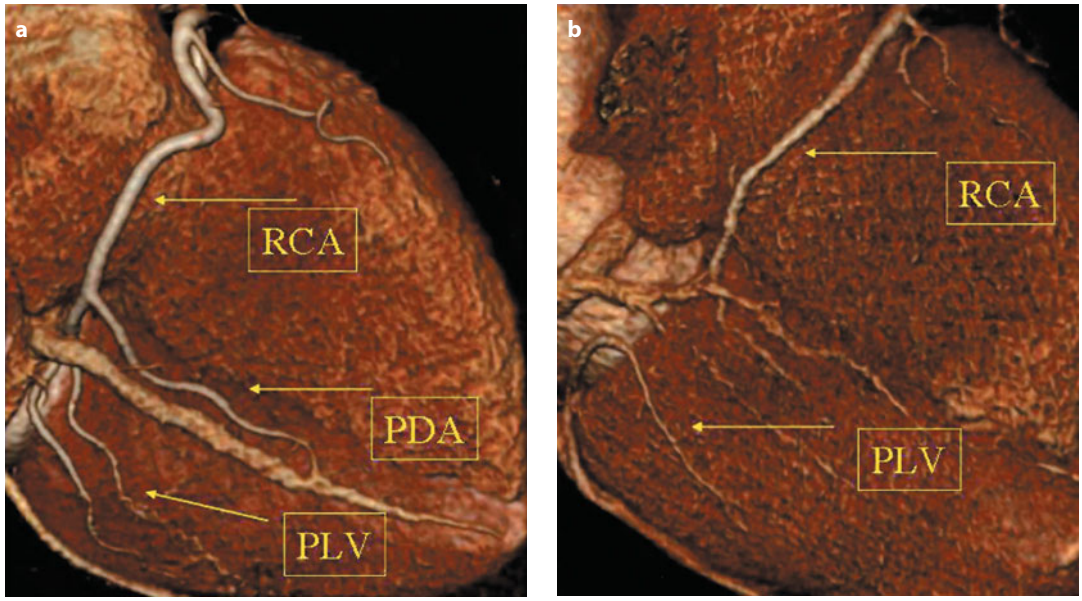

Fig. 1.7 a Right-dominant circulation. **b** Balanced circulation. *RCA* Right coronary artery, *PLV* posterolateral branches, *PDA* posterior descending artery

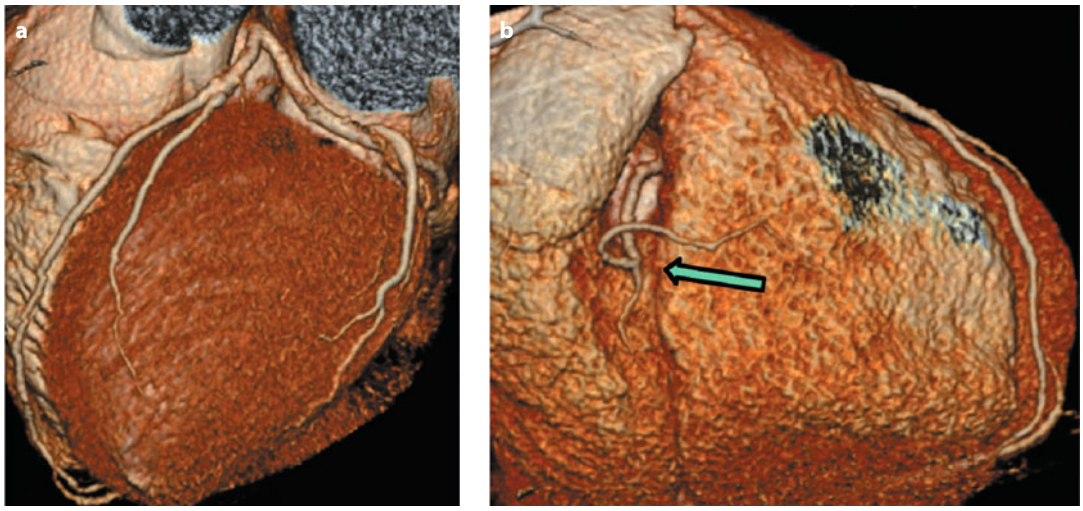

Fig. 1.8 a Left-dominant circulation. The left anterior descending and circumflex arteries are hypertrophic. **b** The right coronary artery (*arrow*) is hypoplastic and branches derive from the acute marginal branch

two arteries depends on the size of the artery from which they derive; that is, the DIAG branches will be of larger caliber than the OM branches when the LAD is more developed than the LCx, while the OM branches will be more developed if the caliber of the LCx is larger.

If the RCA is highly developed, its distal branches (PDA and PLV), in addition to vascularizing the right ventricle, will also perfuse the posterior wall of the left ventricle. In other cases, including right-dominant circulation, the PLV are poorly developed and the great part of the left ventricle is perfused by the LCx (Fig. 1.7).

Finally, the RCA can be hypoplastic, giving rise only to the conus artery after a single AM branch (Fig. 1.8).

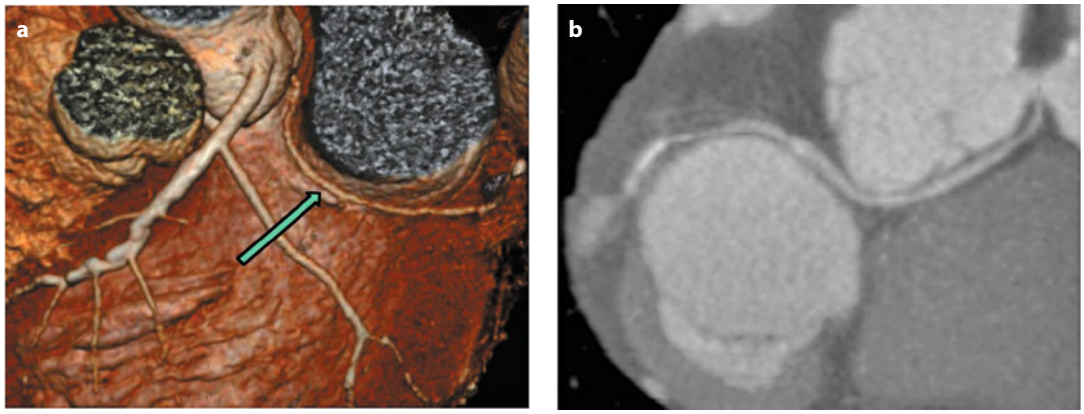

Fig. 1.9 Anomalous origin of the left circumflex artery from the right coronary artery. **a** In 3D view, the anomalous vessel (*arrow*) runs between the aorta and the pulmonary artery. **b** In 2D view, the origin and anomalous and tortuous course of the vessel are visible

These anatomic variations are normal and are not related to ischemic damage.

In the presence of atherosclerotic stenosis in a small vessel, the ischemic portion of the myocardium will be correspondingly small. However, when atherosclerosis develops in a main vessel of greater caliber, especially in the proximal segments, the clinical symptoms will be important and the ischemic area large.

The classical definition of single-, double-, or triple-vessel disease, referring to the number of vessels with critical stenosis, is tightly correlated with the prognosis and with therapeutic planning; nevertheless, the presence of coronary stenosis must be assessed in the context of the global coronary anatomy. Two-vessel coronary disease is similar to three-vessel disease if the third vessel is a hypoplastic or small artery rather than atherosclerotic.

1.5 Anomalous Coronary Arteries

An anomalous coronary artery can be found in 0.64–5.60% of patients who undergo coronary angiography (Fig. 1.9). Some of these variations have no clinical relevance, while others may represent an important pathology.

Separate origins of the RCA and conus artery occur in 40–50% of the cases and a separate origins of the LAD and LCx in 1%. The most important anomaly is a LM artery originating from the right sinus of Valsalva or from the RCA. The course between the pulmonary artery and the aorta can be the cause of vessel compression, and therefore of ischemia and sudden death, during or following physical effort. The same is true when the LAD originates from the RCA or from the right aortic sinus. By contrast, a circumflex artery originating from the RCA has no clinical consequences, because of its posterior course.

Some congenital cardiopathies are often associated with anomalous coronary arteries.

For example, in the tetralogy of Fallot, an anomalous coronary artery is present in 9% of the cases. The most common variation is a great conus artery, an anomalous LAD originating from the RCA or right sinus of Valsalva.

In transposition of the great vessels (D-type), the most frequent (60% of the cases) anomaly is a RCA that originates from the posterior surface of the right aortic sinus and a LAD originating from the posterior surface of the left aortic sinus. In 20% of the cases, the circumflex artery arises from the RCA. In 3–9% of the cases, the RCA arises from the left aortic sinus and the LCA from the right sinus or there is a single coronary artery that takes off from the right or left sinus of Valsalva; an intramyocardial course is frequent.

In the L-type transposition, the coronary arteries can derive from the originating sinus or from

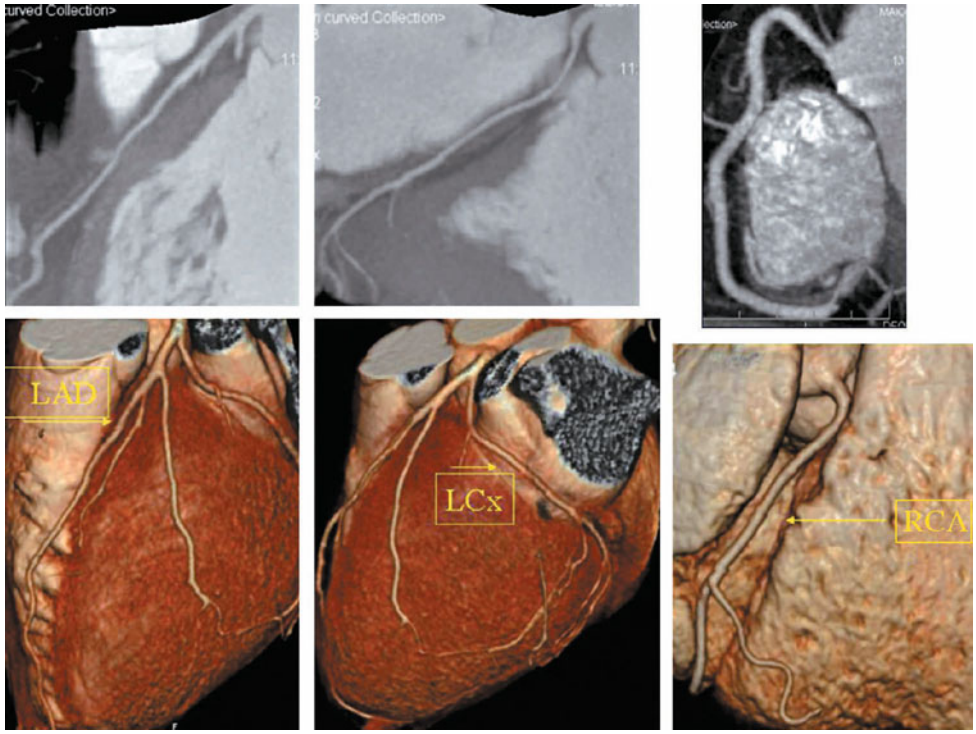

Fig. 1.10 Evaluation of the coronary anatomy with multi-slice computed tomography. *RCA* Right coronary artery, *LAD* left anterior descending artery, *LCx* left circumflex artery

the perfused ventricle. In this case, the RCA perfuses the left ventricle on the right side and divides into the LAD and LCx, and the LCA runs in the interventricular groove similar to the RCA.

The anomaly of one or more coronary arteries arising from the pulmonary artery is seen in 0.4% of patients with congenital cardiopathies.

The most frequent anomalous coronary artery is the LAD originating from the pulmonary artery (Bland-White-Garland syndrome).

Further coronary anomalies are aneurysms and fistulas. Aneurysm is an expansion of the coronary diameter by at least 1.5-fold more than an adjacent segment. Coronary fistulas are communications between the coronary arteries and the cardiac cavities or great vessels: these can be congenital or acquired following thoracic traumas, electrocatheter implantation, endomyocardial biopsies, etc. The most frequent location is the RCA (55%), LCA (35%), or both (5%); in 40% of these patients, the fistula is in the right ventricle, in 26% in the right atrium, and in 17% in the pulmonary artery.

1.6 Factors Determining Coronary Artery Size

Numerous independent factors, including age, sex, body surface area, physical activity, and some pathologies, influence the caliber of the coronary arteries.

For instance, with increasing age there is a reduction of the caliber of the coronary vessels, whereas in patients with myocardial hypertrophy the arteries are of increased caliber.

Generally, in females, the coronary arteries are narrower than in males, probably due to the difference in body surface area. The reduction in the caliber of the coronary arteries that occurs with age has many explanations: firstly, there is a high prevalence of concentric atherosclerosis (not visible with coronary angiography), which causes a homogeneous reduction of the arterial lumen. In most elderly subjects there is also subendothelial and medial hypertrophy. Angiographic examination of

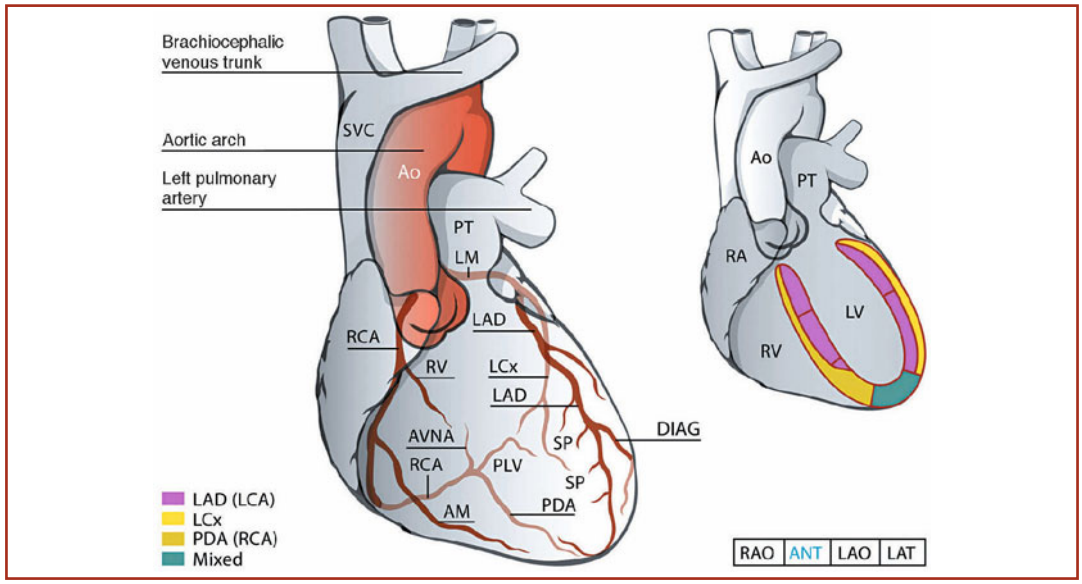

Fig. 1.11 Angiographic evaluation of the coronary circulation; anterior (*ANT*) view. The classification used by the BARI Study Group Investigators is in parentheses. *RCA* Right coronary artery (1), *RVB* right ventricular branches (10), *AM* acute marginal branches (10), *PDA* posterior descending artery (4), *PLV* posterolateral branches (5), *AVNA* atrioventricular nodal artery, *LCA* left coronary artery, *LM* left main artery (11), *LAD* left anterior descending: first segment (12), second segment (13), third segment (14), *SP* septal branches (*17*), *DIAG* diagonal branches (15, 16, 29), *LCx* left circumflex artery: first segment (18), second segment (19), third segment (19a), *OM* obtuse marginal branches (20–22), *Ao* aorta, *LV* left ventricle, *PT* pulmonary trunk, *RA* right atrium, *RV* right ventricle

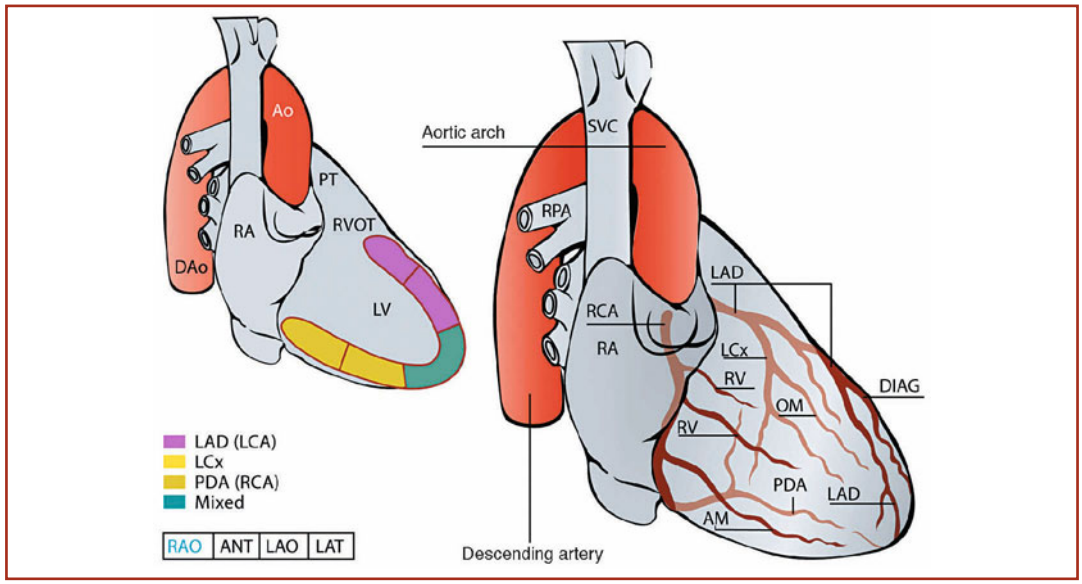

Fig. 1.12 Angiographic evaluation of the coronary circulation; right anterior view (RAO). *RCA* Right coronary artery, *RV* right ventricular branches, *AM* acute marginal branches, *PDA* posterior descending artery, *PLV* posterolateral branches, *LM* left main artery, *LAD* left anterior descending artery, *DIAG* diagonal branches, *LCx* left circumflex artery, *OM* obtuse marginal branches, *Ao* aorta, *Dao* descending aorta, *LV* left ventricle, *PT* pulmonary trunk, *RA* right atrium, *RPA* right pulmonary artery, *RVOT* right ventricular outflow tract, *SVC* superior vena cava

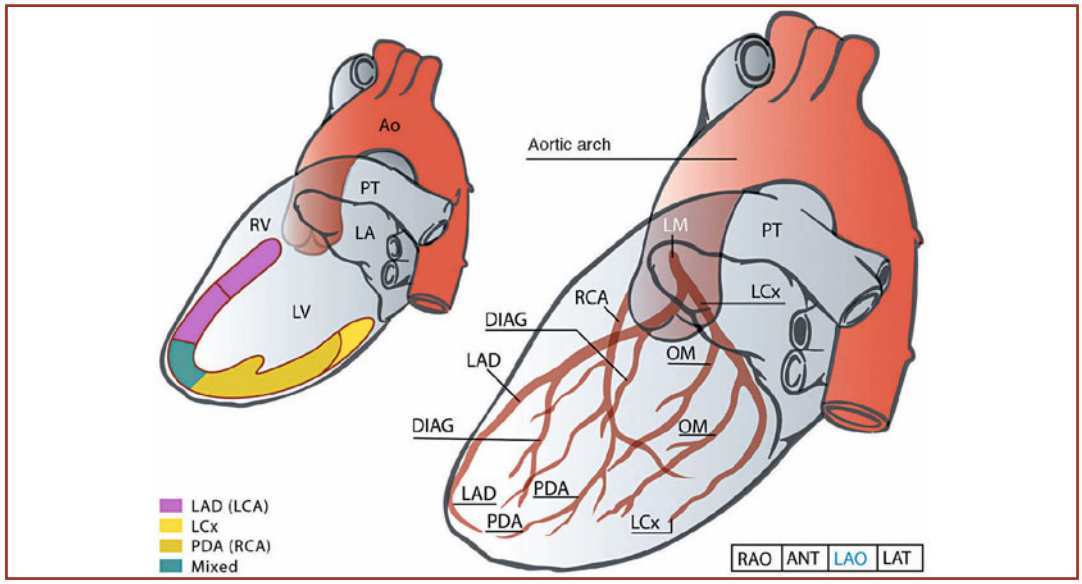

Fig. 1.13 Angiographic evaluation of the coronary circulation; left anterior oblique (LAO) view. *RCA* Right coronary artery, *RV* right ventricular branches, *PDA* posterior descending artery, *LCA* left coronary artery, *LM* left main artery, *LAD* left anterior descending artery, *DIAG* diagonal branches, *LCx* left circumflex artery, *OM* obtuse marginal branches, *Ao* aorta, *LA* left atrium, *LV* left ventricle, *PT* pulmonary trunk, *RV* right ventricle

the diameter of the coronary arteries often requires the use of nitrates to resolve vasospasm; however, with increasing patient age there is a reduction of the effects of nitrates. Furthermore, reduced physical activity and a prevalence of connective tissue in the myocardium are associated with a reduction in the caliber of the coronary arteries.

Physical exercise is a strong stimulus for increasing the caliber of the vessels and it potentiates the effects of nitroglycerin or endothelial-derived relaxing factor.

Cardiac pathologies that increase work by the heart or produce an increase in coronary flow increase the caliber of the coronary arteries. Thus, in the evaluation of the coronary anatomy it is useful to obtain anamnestic information from the patient.

Figures 1.10–1.13 provide examples of the coronary anatomy, as visualized by computed tomography (Fig. 1.10) or with traditional angiographic projections (Figs. 1.11–1.13), including the cardiac regions perfused by the larger coronary branches.

References

1. Alderman EL, Stadius ML (1992) The angiographic definitions of the Bypass Angioplasty Revascularization Investigation (BARI). Coron Artery Dis 3:1189-1220
2. Libby P, Bonow RO, Mann DL, et al (2008) Braunwald's heart disease: a textbook of cardiovascular medicine. 8th edn. WB Saunders, Philadelphia
3. Pavone P, Fioranelli M, Dowe DA (2009) CT evaluation of coronary artery disease. Springer-Verlag, Milan
4. Baim DS (2006) Grossman's cardiac catheterization, angiography and intervention. Lippincott, Williams & Wilkins
5. Topol EJ, Jacobs JJ (2008) A textbook of interventional cardiology, 5th edn. Saunders, Elsevier, Philadelphia

Basic Techniques in the Acquisition of Cardiac Images with CT

2

Paolo Pavone

2.1 Introduction

Computed tomography angiography (CTA) of the coronary arteries is a very fast and the most advanced imaging technique currently available for clinical use. Based on a multi-slice imaging approach together with specialized and dedicated software, CTA "freezes" cardiac movement, thereby acquiring static images of the rapidly moving heart. In addition, the same approach produces contrast-enhanced images of the coronary arteries, by employing a three-dimensional technique with high spatial and temporal resolution. This chapter informs the non-experienced reader about the CTA modalities that allow these images to be acquired. Specifically, the following topics are discussed: (a) the basic concepts of the equipment employed, (b) the technical procedures needed to image the coronary arteries, (c) the modalities for proper reconstruction of the three-dimensional images, and (d) the procedures allowing diagnostic analysis and image reproduction.

2.2 Technical Principles in the Acquisition of Cardiac Images by CT

"Freezing" moving organs has been one of the main goals of CT since its introduction. All of the apparatuses developed thus far are based on a simple principle: an X-ray tube (the same as employed elsewhere in radiology) rotates around the patient, who lies on a radio-transparent bed. A thin, collimated X-ray beam is sent towards the patient from one side while sensors (detectors) are located on the other. The amount of X-ray radiation absorbed by the patient at the anatomic level examined is then computed. Thus, from a simple perspective, CT consists (Fig. 2.1) of a large box, the gantry, which contains a circular track that allows fast rotation of the X-ray tube. On the other side of the tube, positioned along the same track, are the detectors, which rotate synchronously with the X-ray tube. The detectors transform the received signal (i.e., the X-ray beam after it has passed through the patient's body) into a weak but consistent electrical signal that is proportional to the amount of X-rays detected. Accordingly, the greater the absorption of the X-ray beam by the patient, the smaller the number of X-rays that hit the detector, and the weaker the electrical signal transformed and transmitted by the detector. Therefore, the electrical signal created by the detector is a direct measure of X-ray beam absorption. If the beam crosses an area containing bone (e.g., the vertebrae), X-ray absorption will be consistent and a weak signal will be produced by the detector (Fig. 2.2). If an anatomic area containing air (e.g., the lungs) is evaluated, X-ray absorption will be less and a strong, consistent signal will result as very little of the radiation is absorbed by the lungs.

At the same time that information on X-ray absorption is collected by the CT detectors during rotation of the tube around the patient's body, the de-

P. Pavone (✉)
Radiology Department
Casa di Cura Mater Dei
Rome, Italy
e-mail: paolo.pavone@materdei.it

D.A. Dowe, M. Fioranelli and P. Pavone (eds.), *Imaging Coronary Arteries*,
DOI: 10.1007/978-88-470-2682-7_2, © Springer-Verlag Italia 2013

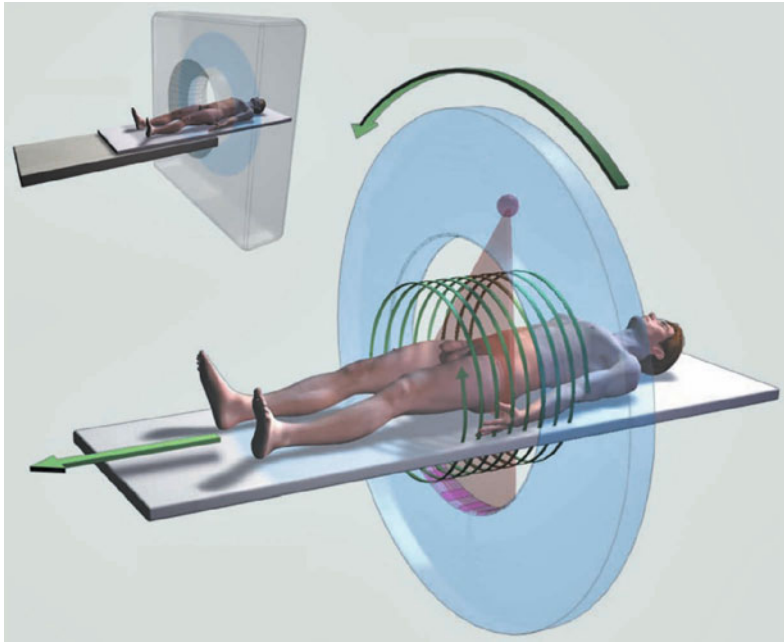

Fig. 2.1 Computed tomography (CT) equipment: basic principles. (Reproduced from Brenner and Hall, 2007. 2008 Massachusetts Medical Society, with permission)

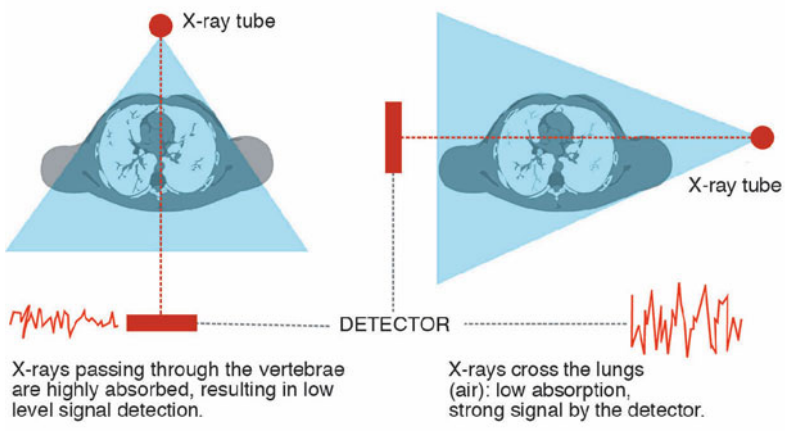

Fig. 2.2 X-ray absorption and signal detection. X-ray absorption is higher or lower depending on the anatomic area crossed by the X-rays. For example, when X-rays pass through the strongly absorbing vertebrae, the detector receives a weak signal. When they pass through the lungs, there is less absorption and the detector receives a much stronger signal

tectors are also continuously and rapidly sending electrical signals to a computer. In the process, these weak but significant electrical signals are immediately transformed into digital data that can be analyzed by the appropriate software. Complex reconstruction algorithms ultimately produce a series of diagnostic images, which are displayed on the console monitor and are thus readily accessible by the clinician.

As simple clinical users, it is not necessary to understand the mechanics of these analyses. It is important, however, to acknowledge those scientists who have been able to resolve the numerous technical problems such that CT image quality has constantly improved. Of interest is that the "inventor" of CT, Sir Hounsfield, succeeded in his efforts thanks in part to the Beatles, since EMI Records financed CT research and the construction of the first "commercial" CT unit. The volumetric (spiral) revolution was a product of the work of Willi A. Kalender. Due to these results and those of related scientific activities, today, CT is used almost as easily as digital photography. Indeed, the acquisition principles are the same: in CT, X-rays

are absorbed by the anatomic region of interest; in digital photography, the brightness of the object is assessed by a kind of detector, the CCD (charge-coupled device), such that the light signal is transformed into numerical (digital) information.

2.3 From Conventional to Spiral CT

The speed of data acquisition in CT depends on two different factors: how fast the tube rotates around the patient and the amount of information that can be analyzed at the same time. Early CT machines needed 18–20 s for a single rotation; thus, the waiting time, in which the tube returned to its initial position ready to begin a new rotation, was as long as 1 min. A revolution in CT imaging of the abdomen occurred in the early 1980s, with a tube able to rotate around the body in 2 s, thereby minimizing all artifacts arising from motions of the abdominal organs. As a result, excellent static images of the liver, pancreas, and adjacent vessels could be obtained.

The next step was the introduction of spiral systems, in which the tube is able to move freely in the track contained in the gantry and does not return to its initial position after each rotation. In these machines, introduced in the early 1990s, the electrical power that supplies the X-ray tube is transmitted along the same rotational track, thus avoiding both the need for long cables and a return to the start position after each rotation. "Spiral" refers to the fact that, once a continuous rotation of the tube around the patient is started, movement of the bed along the longitudinal axis creates a spiral acquisition of images along the human body (Fig. 2.1) instead of the axial images acquired in conventional CT. There is dramatic improvement of image quality with spiral CT in terms of speed of data acquisition and the consistency of the diagnostic information. This is due to the fact that images are not acquired on a single imaging plane (axial); rather, data representative of an entire volume are reconstructed on the axial, coronal, sagittal, and curved planes of the target organ. The information provided by these three-dimensional images facilitates diagnostic evaluation of the internal organs of the human body. Moreover, the development of spiral CT allowed the development of other techniques, such as virtual endoscopy and CTA, which have become routine tools in clinical practice.

2.4 From Spiral to Multi-slice CT

Despite the advances made with the introduction of spiral CT, the acquisition times were still too long to allow cardiac imaging. The rotation time of the tube was about 1 s, not short enough to "freeze" cardiac movement. Moreover, the need remained to acquire more data within the same time frame, in order to include the anatomic area surrounding the heart. With multi-slice CT (MSCT) (Fig. 2.3), which became commercially available at the beginning of this century, an increase in the speed of data acquisition was achieved. The principle of MSCT is simple: in conventional CT, a collimated X-ray beam is emitted and data are collected by a row of detectors located on the other side of the patient, after attenuation of the beam through his or her body. In MSCT, there is a large data-acquisition system, composed of an array of detectors arranged in multiple parallel rows along the longitudinal axis. The larger collimation of the X-ray beam is such that all of the detectors are "hit" at the same time, allowing simultaneous evaluation of a larger anatomic area.

The first systems used in cardiac imaging had four rows of detectors, but the real clinical revolution in cardiac imaging came with the development of machines with 16 detector rows, as they were able to generate images of the coronary arteries with limited artifacts and improved resolution.

Currently, the most widely employed systems have arrays of 64 detector rows, although newer systems with 128, 256, and 320 detectors have since become available. It is easy to understand why the speed of acquisition is proportional to the number of detectors. Coverage of an anatomic volume such as the heart requires a certain number of rotations of the tube around the patient. Clearly, the larger the anatomic area covered by the detector rows, the fewer the number of rotations needed (Fig. 2.4).

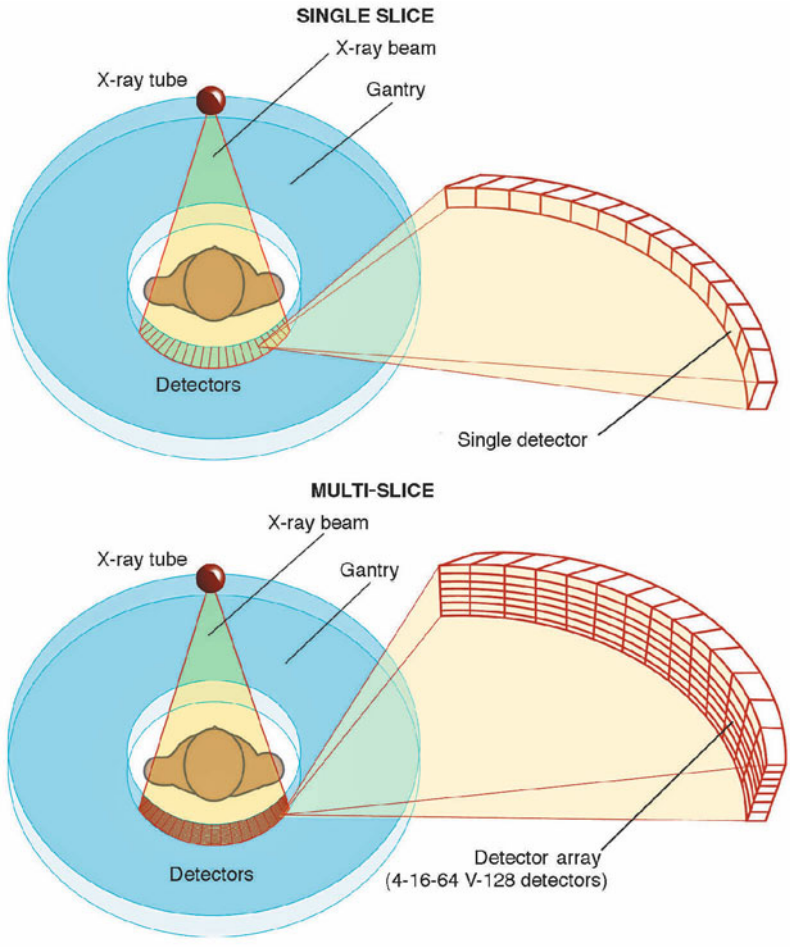

Fig. 2.3 Single slice and multi-slice (multi-row) detector CT

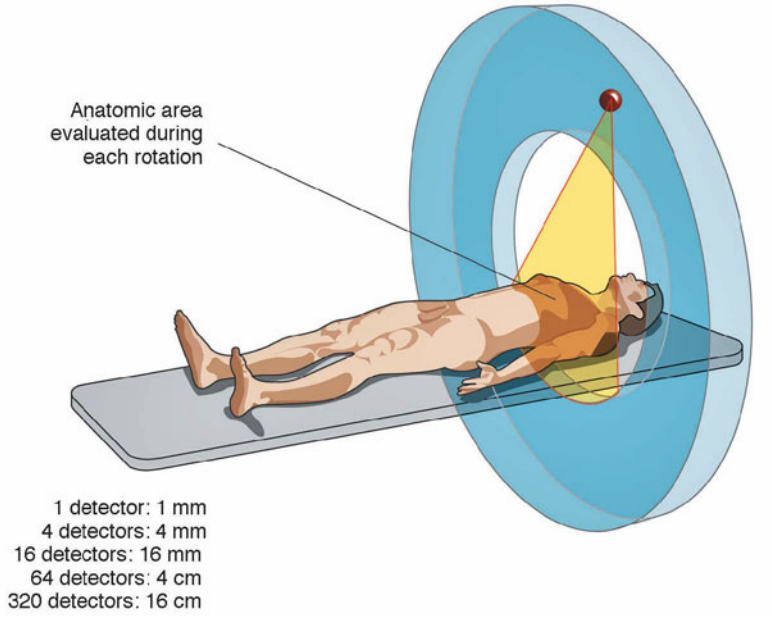

Fig. 2.4 Anatomic area evaluated in a single rotation of the X-ray tube. In MSCT, the higher the number of detectors, the wider the anatomic area evaluated during each rotation of the X-ray tube

2.5 Detector Number and Cardiac Imaging

It is worth emphasizing once more that the number of detectors used in MSCT corresponds to an array of defined width. The volume simultaneously evaluated by the X-ray beam equals the width of the detector array. In a 64-detector-row machine, the detector width and the anatomic area to be explored in a single rotation is in each case 4 cm. Thus, to fully cover the anatomic area of the heart (15–20 cm), four to five rotations are needed during each phase of the cardiac cycle (using cardiosynchronization, as discussed below). With 128 detectors, the number of rotations is reduced by one half, while with 320 detector rows it may be possible to evaluate the entire heart in a single rotation. It should be noted that with 320 detector rows the width of the volume acquired in one rotation corresponds to 16, not 20 cm, due to corrections needed for the so-called cone beam artifact. One rotation, carried out in the telediastolic phase of the cardiac cycle, allows for the simultaneous acquisition of data covering the entire heart. However, multi-cycle images of the heart can also be acquired in a single rotation, with the data reconstructed in the different cardiac phases.

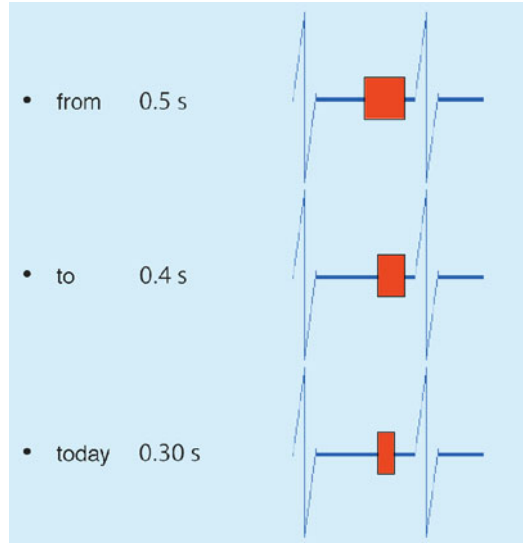

Fig. 2.5 Rotation time of the X-ray tube: during cardiac-gated image acquisition. The width of the red area in telediastole represents the imaging window (time) for data acquisition: the shorter the acquisition time, the fewer the motion artifacts

2.6 Temporal Resolution in Cardiac Imaging

Together with progress achieved by MSCT regarding the simultaneous acquisition of more data, efforts have been made to reduce the rotation time of the X-ray tube. This technical parameter is of utmost importance, as it represents the real temporal resolution of cardiac CT. In fact, even with the largest detector array (i.e., 320), it would not be possible to "freeze" images of the heart if the rotation time of the X-ray tube was slow (e.g., 1 s, as was the case with the first generation of spiral scanners). In other words, it is not enough to simultaneously obtain as much data as possible; rather, data acquisition must be very fast if the goal is to generate consistent cardiac images.

The rotation time of early MSCT equipment, 0.5 s, was too slow to completely "freeze" cardiac movement. Since the temporal resolution is equal to half of the rotation time, with 250 ms significant artifacts in the diagnostic images were produced and the images were of poor quality.

The rotation time of the X-ray tube has continuously improved in more recent equipment and currently ranges from 0.4–0.35 s to 0.3–0.27 s (temporal resolution < 150 ms). As would be expected, the faster rotation times have yielded cardiac images of much higher quality, greater reliability, and improved accuracy, as confirmed by world-wide clinical experience. The reason for this improvement lies in the fact that the width of the imaging "window" (Fig. 2.5) in the telediastolic phase (during which the heart is almost completely still) is limited; therefore, the faster the data are acquired, the fewer the movement artifacts.

Another approach to improve temporal resolution is the use of two perpendicular X-ray tubes. In dual-source technology, two different X-ray tubes are installed 90° to each other on the same rotational track, with two perpendicular detector